Ceramics International **24** (1998) 125–133

PII: S0272-8842(97)00041-2
0272-8842/97 $17.00+.00

Effect of Processing Variables on Warping Behaviours of Injection-Moulded Ceramics

Wenjea J. Tseng & Dean-Mo Liu

Materials Research Laboratories, Industrial Technology Research Laboratories, Chutong, Hsinchu 31015, Taiwan

(Received 3 June 1997; accepted 3 July 1997)

Abstract: The warpage behaviours of injection-moulded ceramics were investigated through a designed, factorial experiment. The warpage was found proportional to the mould temperature, and was reduced as a prolonged cooling time was concurrently applied. The residual stresses arising from the nonuniform temperature distribution during the cooling stage of the moulding process were suspected as the main cause, and a model experiment by artificially introducing a differential cooling rate across the moulding thickness confirmed the hypothesis. The differences in warping behaviours between the injection-moulded ceramics and plastics, as well as the implication of the moulded microstructure to the warpage, are discussed. © 1997 Elsevier Science Limited and Techna S.r.l.

1 INTRODUCTION

Ceramic injection moulding offers a near-net-shape fabrication route for making complex-shaped ceramic components in a large production volume. To obtain injection-moulded parts cost-effectively, dimensional accuracy and shape fidelity have to be assured. In particular, the shrinkage-related defects, such as the warping deformation, must be eliminated or minimised to a satisfactory level, otherwise the near-net-shape process would not be truly meaningful.

For the plastic injection moulding, relevant studies concerning this issue are extensive. It has been pointed out that the asymmetrical residual stress is the primary cause for the warpage deformation.[1–4] The source of the residual stress is considered to mainly result from the nonuniform thermal contraction during solidification, as well as from the flow of plasticated melts during the die filling. In the literature, however, little attention has been devoted to this subject in ceramic injection moulding. Zhang and Evans reported that the shape distortion occurred when green mouldings were subjected to annealing treatments at a temperature below the glass transition temperature of binders.[5,6] The deformation was also found during thermal debinding,[7] especially at a temperature range where the rate of binder loss was notable. Recently, Zhang *et al.*[8] revealed that the warpage was influenced by the morphology of the starting powder, and by the binder orientation as well. They concluded that plate-like particles might orient themselves under the shear forces during the moulding stage, and induced binder orientation consequently, which would then restrict the relaxation of the green mouldings when subjected to the post-moulding annealing. In their study, the curve deformation was found to be unrelated to the varying injection pressures and melt flow-rates.

Nevertheless, the details about the relative significance of processing factors to the warpage behaviours of the ceramic injection moulding remain unclear. One might think that the complex interaction and correlation effects involved in the injection moulding process inhibit full understanding of the underlying mechanisms. Therefore, the current study aims at providing such information by designing a statistically factorial $L_{16}2^{15}$ experiment to unveil the dominate variables for the formation of the warpage on injection-moulded ceramics.

2 EXPERIMENTAL PROCEDURES

The experimental design and selected levels are shown in Tables 1 and 2. Eight principal factors and seven interactive factors were arranged in an orthogonal array and the resultant responses were analysed by the analysis of variance (ANOVA) and the F-test. The moulding experiment was conducted by a microprocessor controlled injection-moulding machine (BA 250/50 CDC, Battenfeld, Austria). Submicrometer zirconia powders (HSY-3.0, Daiichi Kigenso Kagaku, Japan) with a relatively spherical shape were used for the study. Low molecular weight organic binder composed of paraffin wax, vinyl acetate polymer and stearic acid in varying weight ratios of 5:5:1 and 7.5:2.5:1 were used as major ingredient, minor ingredient and lubricant, respectively.[9] The mould consisted of two halves where one side was connected to the nozzle of the injection unit and the other half to the ejector system where samples were demoulded by the pin ejectors. The parallelepiped mouldings with dimensions of 4 × 5 × 60 mm were prepared, stored in a controlled humidity of 55–60% relative humidity (RH) at room temperature for three days, debound at 600°C in air atmosphere in a rate of 20°C h^{-1}, and followed by sintering at 1500°C for 1 h.

Table 1. The selected controlling factors and their experimental levels for evaluating warpage deformation of ceramic mouldings

Factors	Level 1	Level 2	Interaction*
A. Solid loading	50 vol%	57.5 vol%	
B. Wax/polymer ratio*	50/50	75/25	
C. Holding pressure	60 MPa	120 MPa	
D. Hold pressure time	5 s	20 s	
F. Mould temperature	38°C	48°C	
G. Cooling time	15 s	45 s	
H. Ejection speed**	20%	60%	
I. Ejector force	5.3 kN	8.8 kN	

*Weight ratio.
**Nominal speed specified by the injection machine.

The warping deformations were measured by a linear variable differential transformer (LVDT) where long-axis direction of the mouldings was considered most prone to the curve deformation. The moulded bars were placed onto an optically flat surface and then the LVDT tip was adjusted to contact with the upper surface of mouldings. It applied a small force ensuring a good physical contact and the contact stress was not significant enough to buckle the moulded bars. Dimensions measured by placing both sides of the moulding surfaces (i.e. sample surfaces facing the nozzle and the ejector sides) to contacting with the LVDT were determined. The warpage was then calculated from the dimensional measurement by

$$\text{warpage}(\%) = (h_e - h_n) \times 100/l \quad (1)$$

where h_e and h_n are the dimensions measured from placing the ejector and nozzle sides of the moulded samples to face the LVDT, respectively; and l is the sample length. Figure 1 shows the arbitrarily chosen positive and negative warpage values, indicating directions of the warping deformation. We assumed that the warpage along axial direction was symmetrical about the moulding's centre, and the average warpage was determined from measurements of 12 to 20 samples.

The moulded samples were then placed in alumina holders for the thermal pyrolysis and the sintering. The samples were placed such that both of the dimension-measuring surfaces were perpendicular to the holder surface for avoiding

Table 2. The orthogonal array of the statistical $L_{16}2^{15}$ experiment and the resulting experimental response

Factor	F	C	C F	A	B	G	F G	D	D F	C D	H	I	F I	B H	A H	Response
Runs\Column	1	2	3	4	5	6	7	8	9	10	11	12	13	14	15	Warpage (absol. %)
1	1	1	1	1	1	1	1	1	1	1	1	1	1	1	1	0.25
2	1	1	1	1	1	1	1	2	2	2	2	2	2	2	2	0.39
3	1	1	1	2	2	2	2	1	1	1	1	2	2	2	2	0.20
4	1	1	1	2	2	2	2	2	2	2	2	1	1	1	1	0.21
5	1	2	2	1	1	2	2	1	1	2	2	1	1	2	2	0.18
6	1	2	2	1	1	2	2	2	2	1	1	2	2	1	1	0.16
7	1	2	2	2	2	1	1	1	1	2	2	2	2	1	1	0.30
8	1	2	2	2	2	1	1	2	2	1	1	1	1	2	2	0.20
9	2	1	2	1	2	1	2	1	2	1	2	1	2	1	2	0.38
10	2	1	2	1	2	1	2	2	1	2	1	2	1	2	1	0.46
11	2	1	2	2	1	2	1	1	2	1	2	2	1	2	1	0.32
12	2	1	2	2	1	2	1	2	1	2	1	1	2	1	2	0.47
13	2	2	1	1	2	2	1	1	2	2	1	1	2	2	1	0.75
14	2	2	1	1	2	2	1	2	1	1	2	2	1	1	2	1.32
15	2	2	1	2	1	1	2	1	2	2	1	2	1	1	2	0.26
16	2	2	1	2	1	1	2	2	1	1	2	1	2	2	1	0.48

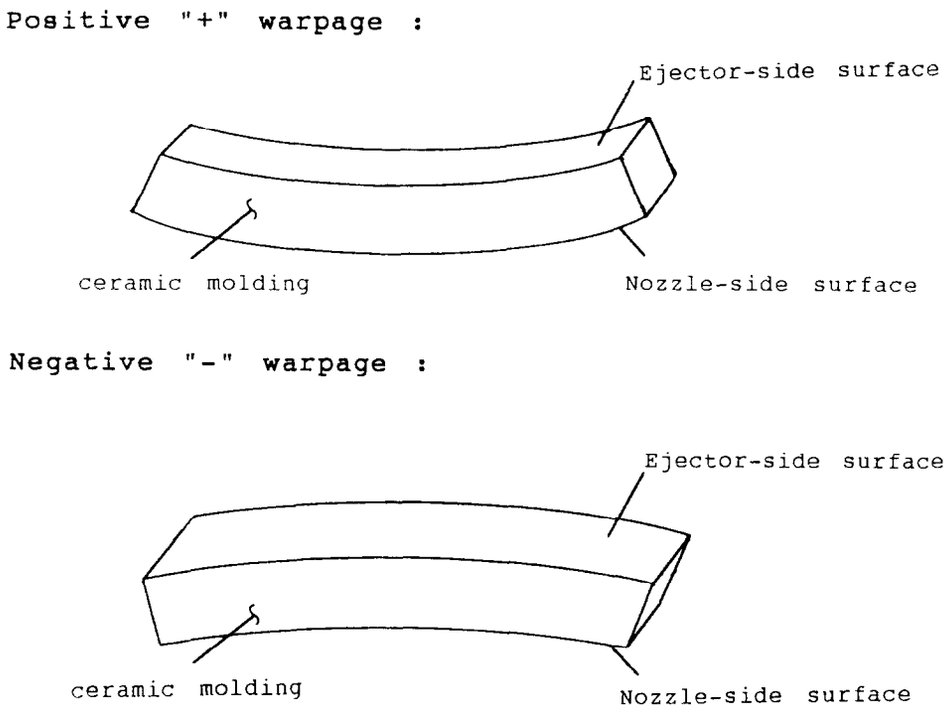

Fig. 1. The direction of warpage deformation (the "+" and "−" warping directions are chosen arbitrarily and are consistent throughout the content of this paper).

possible friction arisen from the physical contact. The samples were also shielded from direct radiation from the heaters in order to ensure a better temperature uniformity and to minimise temperature gradients between surface and core of the moulded samples. The typical reproducibility of measured curve deformations was within $\pm 10\,\mu$m, corresponding to a maximum of $\pm 0.04\%$ warpage at the sintered state.

3 EXPERIMENTAL RESULTS

3.1 Process variables influencing sintered warpage

Table 2 shows that varying moulding and material parameters result in warpage variations ranging from 0.16 to 1.32% in absolute values. The ANOVA and the F-test results further revealed that the mould temperature was the most crucial factor in determining the sintered warpage, with a contribution rate over 31% (Table 3(AB)). The statistical computation in Table 3(B) shows that the mould temperature of the lower level is favourable in reducing the deformation. The warpage varied proportionately with the increased mould temperature.

The interaction between the mould temperature and the cooling time followed the mould temperature as the second notable variable, contributing over 13%. Likewise, the factor interaction of the mould temperature and the hold pressure was also significant, contributing near 8%. It was found that the lower mould temperature coupled with the longer cooling time and the higher hold pressure would lessen the warpage.

Table 3(A). The significance of process variables from the ANOVA and the F-tests

Source of variation	Sum of squares	Degree of Variance freedom		F	Contribution @(%)	
F	85849	1	85849	28.55	31.50	**
FG	38025	1	38025	12.64	13.31	*
A	28561	1	28561	9.50	9.72	*
CF	23562	1	23562	7.84	7.82	*
B	20306	1	20306	6.75	6.58	*
DF	13806	1	13806	4.59	4.11	
C	12996	1	12996	4.32	3.80	
D	12544	1	12544	4.17	3.63	
G	9312	1	9312	3.10	2.40	
e	18044	6	3007		17.15	

* Significant at the 0.05 level.
** Significant at the 0.01 level.

Table 3(B). The ANOVA table summarising the effect of levels on the statistically computed warpage values

Factor	Average (level 1–%)	Average (level 2–%)
F	0.22610	0.54808
C	0.32445	0.44973
CF	0.47143	0.30275
A	0.47995	0.29423
B	0.30879	0.46538
G	0.33407	0.44011
FG	0.49423	0.27995
D	0.32555	0.44863
DF	0.45165	0.32253
CD	0.40934	0.36484
H	0.33819	0.43599
I	0.35330	0.42088
FI	0.38819	0.38599
BH	0.40577	0.36841
AH	0.35440	0.41978

In addition to the effect from the varying moulding parameters, influence of the process variables from the material's perspective was also vital. Both the solid loading and the binder formulation of the feedstocks were significant, with contribution rates of 10% and 7%, respectively. To reduce the warpage, the feedstock with the higher solid loading and the binder formulation with the lower wax to polymer ratio (i.e. the binder formulation contained more polymers) was preferred, yielding a reduced warpage. The total contribution from these found factors represents near 70% of the overall contribution, indicating a majority for minimising the warpage. Nevertheless, some 17% of the contribution were from factors not chosen in the factorial experiment, suggesting the complex nature of the warpage formation.

3.2 Effect of thermal barrier on warpage behaviour

In view of the fact that the sintered warpage was closely related to the mould temperature and the cooling time, a model experiment was conducted by artificially introducing a differential cooling rate through deliberately placing a thermal barrier onto one side of the mould cavity. The barrier was thought to produce a nonuniform temperature distribution, which in turn, would result in an unbalanced residual stress over the cross-section of the mouldings, and might render a better understanding of the various processing parameters on the warpage formation.

The barrier layer (the material was paper and consisted of glossy coatings on the surface to facilitate easy removal from the moulded samples after demoulding) was placed onto the ejector side of the mould cavity prior to the moulding process. The warpage deformations of the moulded "green" bars (referred to as layered mouldings), as well as the sintered specimens, were both measured. The thermal conductivity of the barrier was about $0.18\,W\,m^{-1}K^{-1}$ (similar to that of the binder species, c.f. the Appendix) and had a thickness of $300\,\mu m$. Since the thermal conductivity of the zirconia ceramics presented a substantially larger value than that of the binders, the plasticated melt near the ejector side experienced a cooling rate significantly lower than the other side of cavity. The thermal conductivity of the layered mouldings with heat flows in a direction perpendicular to the stacking direction is approximated by

$$\kappa = \frac{\kappa_1 \kappa_2}{\nu_1 \kappa_2 + \nu_2 \kappa_1} \tag{2}$$

where κ_1 and κ_2 represent the conductivities of two individual layers and ν the volume fraction of respective layer. Hence, for the layered mouldings (the feedstock consisted of the solid loading of 57.5%, and the wax/polymer ratio of 50/50) the conductivity was approximately $0.50\,W\,m^{-1}K^{-1}$, a value falling within the conductivity values of 50% and 57.5% loadings (c.f. the Appendix). The minimum cooling time of the mouldings with the thermal barrier was thus expected not exceeding 13 s, indicating that the cooling time employed in the factorial experiment well exceeded the calculated value. It thus minimised potential errors arisen from influence of other factors not chosen in the factorial experiment.

Figure 2 shows the warpage of the layered "green" mouldings which were moulded at the various mould temperatures and cooling times. Compared to the samples fabricated in the statistical experiment where most of the samples were positively warped, the warpage values were negative for all the layered mouldings. The absolute values of the green warpage were more than twice than that of the non-insulated mouldings, apparently due to the enlarged effect on the differential cooling. It has been reported that, similar to quenching experiment of glass, injection moulded parts often exhibit compressive stresses on the outer surface of mouldings while changing to the tensile stresses as approaching toward the centre of mouldings.[1,10,11] If the stress distribution shows a symmetrical profile with respect to the moulding centre, a balanced overall stress is expected. However, if the differential cooling rates exist, the stress profile would not be symmetrical and hence an unbalanced stress profile is induced. In this case, mouldings have a tendency to warp after ejection in order to reduce the unbalanced state of stress. The idea may be better described when considering

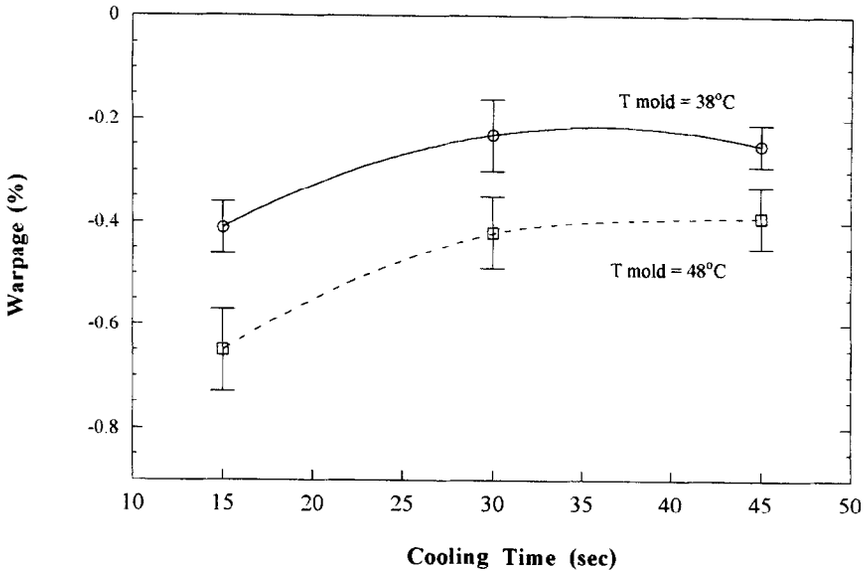

Fig. 2. The warpage of layered green mouldings (i.e. with the thermal barriers during moulding) at various moulding temperatures and cooling times.

a schematic plot shown in Fig. 3, where the development of the residual stresses from the nonuniform cooling is presented. The moulding thickness is imagined divided into separate layers, with an assumption that each layer is virtually independent. In the case that the temperature distribution across the thickness produces a symmetrical profile, as shown in Fig. 3(a), the layers contract freely with the central layer shrinking the most while the outmost layers are chilled instantaneously when contacting with the cold mould surface. The contraction without hindrance among layers produces a symmetrical shape; however, since the imaginary layers are in fact constrained an average "bulk" contraction must be maintained. It then induces residual stresses where the layers near the surface are under compression while balancing tension stresses exist at the centre. Overall stress profile exhibits the symmetrical form across the moulding thickness. On the other hand, for the case where the differential cooling rate exists, the temperature distribution is accordingly changed. The contraction of layers varies and the resulting stress profile is not symmetrical about the centre, as shown in Fig. 3(b). While the ceramic mouldings are still within the cavity (i.e. before ejection) the shrinkage and warpage are concurrently constrained by the cavity wall; yet, stresses are built up within the moulding bodies during the cooling stage instead of undergoing warpage deformation. Upon release from the cavity (i.e. soon after ejection), since the tensile and compressive stresses must be balanced, the mouldings warp instantaneously while the mouldings are still warm, in compliance with the reduction of the unbalanced stresses. This phenomenon may be physically reasoned by recognising that the last molten melt is not positioned at the centre of the layered mouldings, but locates toward the side presenting the slower cooling. The warpage development would terminate as the temperature of mouldings approaching their glass transition temperature. For the case that mouldings were kept within the cavity for a sufficient period of time and with the temperature close to the mould temperature before the ejection, the samples are less warped. The deduction is vindicated by the experimental result shown in Fig. 2, i.e. as the mould temperature increases the warpage becomes more pronounced (approaching toward a more negative value). It hence explains why processes with the lower mould temperature and longer cooling time resulted in the mouldings with the lesser degree of warpage at the green state.

The sintered warpage presented a similar trend as the green mouldings, but with a larger scattering among samples (Fig. 4). The scattering was mostly due to the warpage difference between the samples of the same run where they were moulded at presumably the identical condition. Inspecting the warpage change of individual moulding, it clearly showed that the mouldings which were more seriously deformed at the green state exhibited a larger sintered warpage. The cause for the increased scattering is not clear at present, but we suspect the microstructure of the mouldings plays a significant role.

4 DISCUSSION

Pötsch and Michaeli[1] pointed out that the warpage resulted if the residual stress profile gave rise to an asymmetrical stress distribution. The stress profile

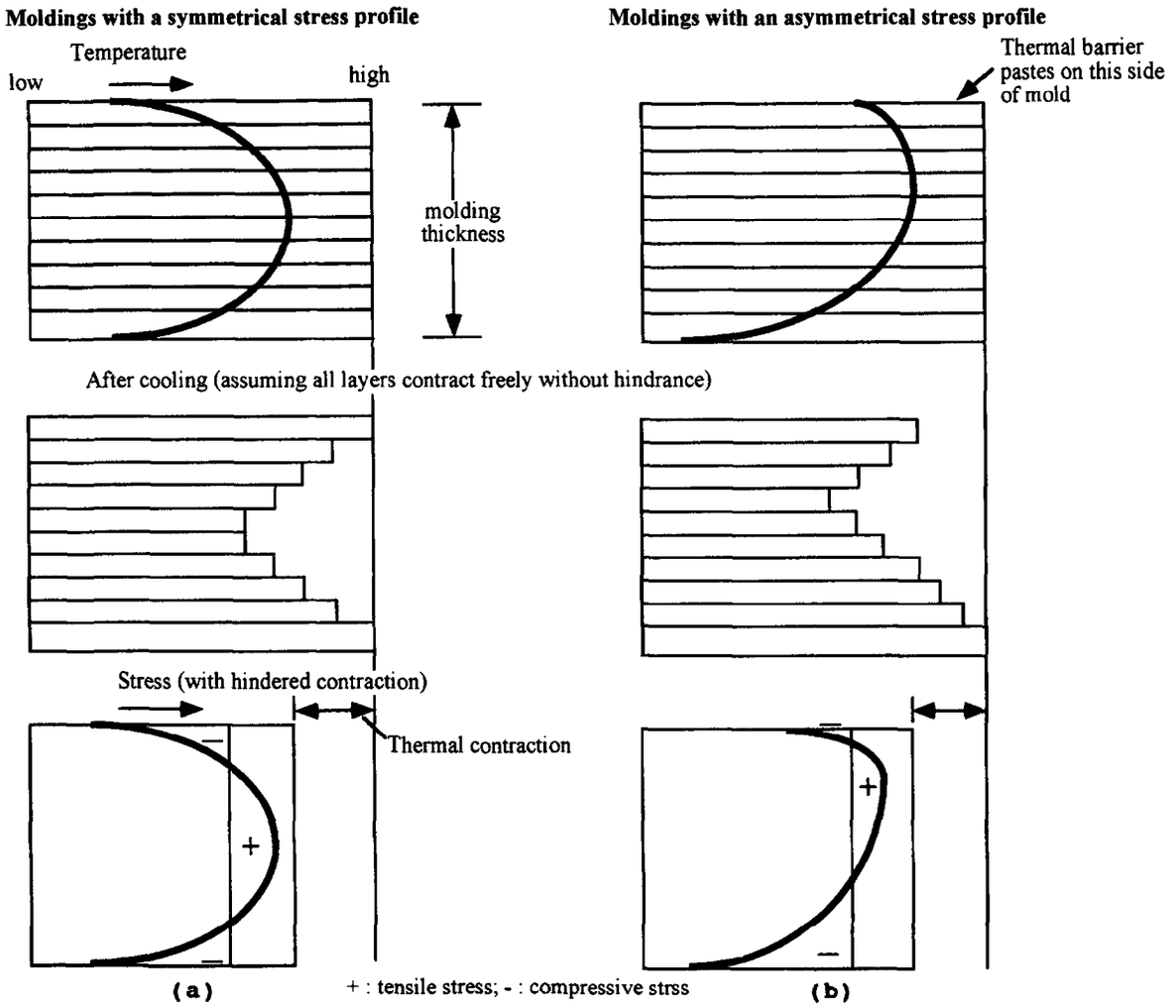

Fig. 3. The schematic plot showing development of the residual stresses during the cooling stage of injection moulding.

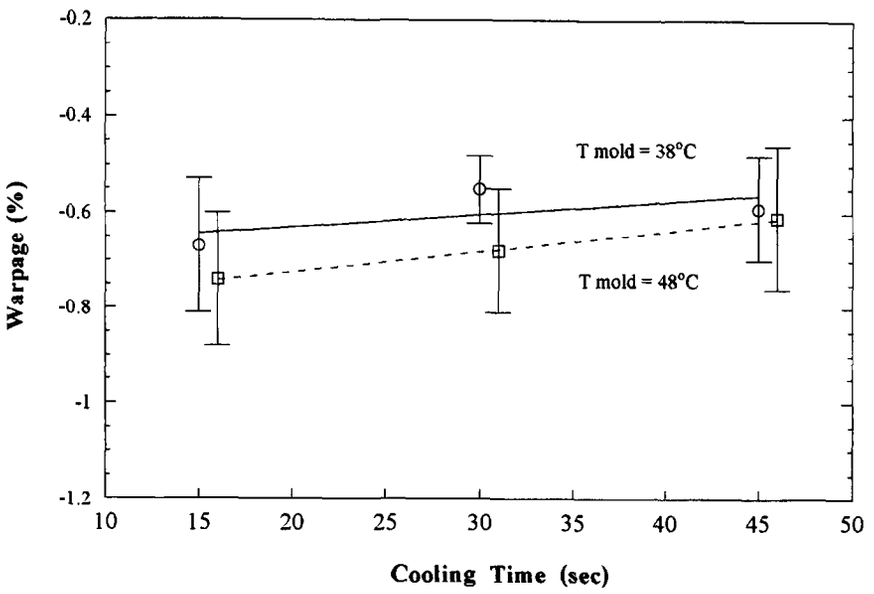

Fig. 4. The warpage of sintered, layered mouldings (i.e. with the thermal barriers during moulding) at various moulding temperatures and cooling times. Notice that the data for the mould temperature of 38 and 48°C are separated for clarification purposes.

is mainly obtained from the superposition of stresses induced from both the constrained thermal contraction during solidification and the stresses originating from the fountain flow, as well as from the overpacking during the filling stage of the injection-moulding process. In particular, the differential cooling rate is considered the main cause for the warpage formation.

There exist notable similarities and differences in warping behaviours of the injection-moulded plastics and ceramics. If the melt temperature were held constant, the lower mould temperature would increase the temperature gradient among "layers" in Fig. 3 for the plastic injection moulding. The increased gradient leads to a larger hindrance between layers and a larger residual stress consequently. It is also normally anticipated that a longer cooling time yields an increased residual stress, mostly because the warmer the ejected mouldings the better the relaxation process is to reduce the stresses. Both injection-moulded plastics and ceramics confirm that the warpage of mouldings is diminished when the residual stresses should in fact become more pronounced. This observation may be explained from the results of our model experiment that even though the magnitude of the residual stress may increase from the change of processing variables, it is the profile of the stresses (i.e. the asymmetrical stress distribution resulted from the nonuniform cooling rates) that determines the warpage the most. The ejected mouldings with the asymmetrical stress distribution are warped immediately in order to reach a more balanced stress profile. The conclusion is identical for both the plastic and ceramic injection mouldings. However, a difference exists between the ceramic and the plastic injection mouldings in the warpage behaviours, i.e. the post-ejection thermal processes (e.g. debinding and sintering) are not necessary for the plastic injection moulding. Since the warmer the ejected samples are the better the relaxation of stress is, a usual practice in controlling the warpage of the injection-moulded plastics is to compress the moulded parts at either the packing stage of the moulding process or after the part ejection (even though the process is best suited for samples with a simple geometry). For the ceramics, the stress built up in the cooling stage of moulding process might be dissipated in the subsequent heating cycle. To confirm this, some samples underwent annealing treatment, and their warpage behaviours were examined. The annealing condition was chosen at a temperature below the glass-transition temperature of the low-melting-point binder species, and the samples were kept at that temperature for 10 h. The annealing time was considered sufficient for releasing more than 90% of the "relievable" residual stresses, as shown in Fig. 5. A reversion in deformation back to the less warped state was found. Even though the warpage of the annealed samples recovered toward the positive side to a significant extent, they yielded a comparatively less warped form; however, a virtually indistinguishable difference on the sintered warpage was found for the mouldings with and without the annealing. The result suggests that the sintered warpage is more dependent on the state of stresses at the green state. The warping deformation after moulding ejection *does* influence the sintered warpage.

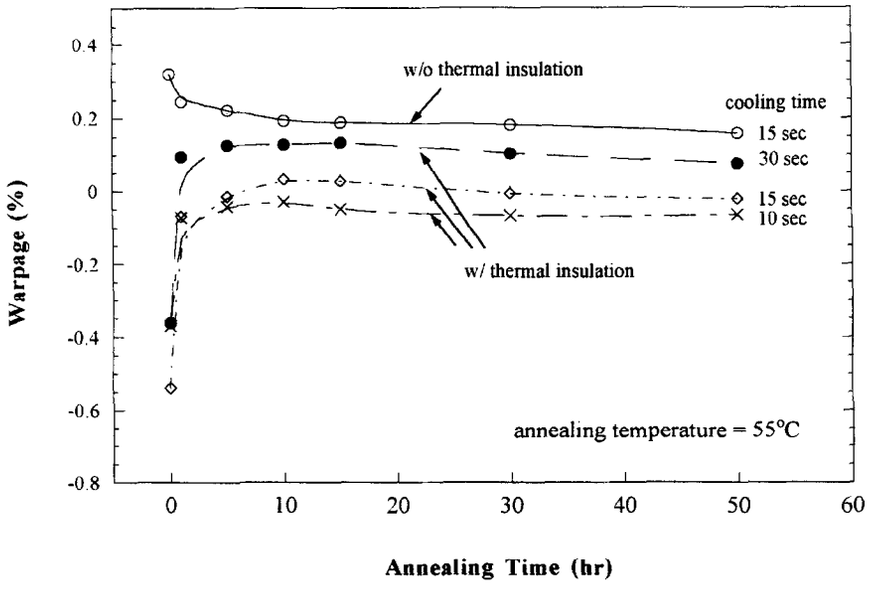

Fig. 5. The warpage profile of the green mouldings annealed for various times.

The underlying mechanisms for the trifling influence of the annealing treatment to the sintered warpage are not well understood at present; however, Liu and Tseng[9] have pointed out recently that microstructure of the injection-moulded samples is apparently agglomerated. Therefore, for the fine starting powders used in the study, the degree of agglomeration to the packing uniformity of the green mouldings, and subsequently to the warping behaviours may need to be further examined. According to Song and Evans,[12] the maximum shear stress during mixing should exceed at least five times the agglomerate strength, in order to obtain a well-dispersed feedstock. If the agglomeration form a constrained network within the mouldings, further stress relaxation may be hindered even when a prolonged annealing is applied, leaving residual stresses to a certain level and subsequently influencing the sintered warpage behaviours. Hindle *et al.*[2] compared the relaxation of residual stresses of the injection-moulded polypropylene (PP) and the short glass-fibre filled polypropylene (GFPP) containing 20 wt% of the fibre. For the GFPP, significant stresses were found remaining after the heat treatment at elevated temperatures, implying that the relatively rigid inclusions form bridges which impede further stress relaxation. Exactly how moulded microstructure (including, for example, dispersion of agglomerates, as well as agglomerate size and strength) influence the warpage requires more experimental analyses; however, it has been discussed previously that minimisation of residual stresses does not necessarily correspond to the reduced warpage. Nevertheless, the moulding with a high level of residual stresses after ejection presents a greater possibility to develop a high distortion if imbalance of stress distribution exists. Therefore, it is anticipated that the green mouldings with a "uniform" microstructure (to an unknown extent which is difficult to quantify at present) and a minimal residual stress are favourable to yield the injection-moulded ceramics with a smaller degree of warpage. The microstructural inhomogeneities may affect moulded samples to a different extent, even though samples are moulded at presumably identical conditions. The warpage scattering, as shown in Figs 2 and 4, might therefore be attributed to the microstructure homogeneity of the mouldings.

The residual stress profiles are also greatly related to the gate design,[3] where the residual stress may change sign depending on the location and injection parameters. In addition, a comparison of different warping directions from the sintered mouldings of the statistical experiment revealed that the design of cooling system of the die may be equally important. However, the objective of this study is obviously not in the mechanical system of moulding technology. In fact, this study shows that the factorial experimentation presents the space to find the optimal processing window to a certain extent without the expensive mould tooling.

5 CONCLUSIONS

The control of mould temperature and cooling time is vital in determining the warpage deformation of the injection-moulded ceramics. The deformation is found proportional to the mould temperature and is diminished as the cooling time increases. The model experiment of the layered mouldings shows that the asymmetrical temperature distribution within the mouldings gives rise to the unbalanced residual stress across the moulding thickness, which in turn, results in shape distortion as the mouldings are released from the constrained mould cavity. Applying the annealing treatment on the green mouldings may recover the dimension but is found not directly related to the sintered warpage. It is speculated that the influence from the microstructural inhomogeneity coupling with the residual stress effect might be the governing mechanisms for the warping behaviours of the injection-moulded ceramics.

ACKNOWLEDGEMENT

The authors are grateful to the Ministry of Economic Affairs, Taiwan, for supporting this research through contract No. 863KG2230.

REFERENCES

1. PÖTSCH, G. & MICHAELI, W., *Injection Molding: An Introduction*. Hanser/Gardner Publications, Inc., Cincinnati, OH, 1995, pp. 127–139.
2. HINDLE, C. S., WHITE, J. R., DAWSON, D. & THOMAS, K., Internal stress, molecular orientation, and distortion in injection moldings: polypropylene and glass-fibre filled polypropylene. *Polym. Engng. Sci.*, **32** (1992) 157–171.
3. PHAM, H. T., BOSNYAK, C. P. & SEHANOBISH, K., Residual stresses in injection molded polycarbonate rectangular bars. *Polym. Engng. Sci.*, **33** (1993) 1634–1643.
4. GREENER, J., General consequences of the packing phase in injection molding. *Polym. Engng. Sci.*, **26** (1986) 886–892.
5. ZHANG, T. & EVANS, J. R. G., Relaxation effects in large injection moulded ceramic bodies. *J. Eur. Ceram. Soc.*, **12** (1993) 51–59.
6. ZHANG, T. & EVANS, J. R. G., The use of a heated sprue in the injection moulding of large ceramic sections. *Br. Ceram. Trans.*, **92** (1993) 146–151.

7. SUNBACK, C. A., COSTANTINI, M. A. & ROBBINS, W. H., Part distortion during binder removal. In *Ceramic Materials and Components for Engines, Proceedings of Third International Symposium*, ed. V. J. Tennery. The American Ceramic Society, Westerville, OH, 1989, pp. 191–200.
8. ZHANG, T., BLACKBURN, S. & BRIDGWATER, J., The orientation of binders and particles during ceramic injection moulding. *J. Eur. Ceram. Soc.*, **17** (1997) 101–108.
9. LIU, D.-M. & TSENG, W. J., *Ceram. Int.*, in press.
10. KOSTIC, B., ZHANG, T. & EVANS, J. R. G., Measurement of residual stress in injection-moulded ceramics. *J. Am. Ceram. Soc.*, **75** (1992) 2773–2778.
11. HUNT, K. N., EVANS, J. R. G., MILLS, N. J. & WOODTHORPE, J., Computer modeling of the origin of defects in ceramic injection moulding—IV. Residual stresses. *J. Mater. Sci.*, **26** (1991) 5229–5238.
12. SONG, J. H. & EVANS, J. R. G., The assessment of dispersion of fine ceramic powders for injection moulding and related processes. *J. Eur. Ceram. Soc.*, **12** (1993) 467–478.

6 APPENDIX: ESTIMATION OF MINIMUM COOLING TIME FOR INJECTION MOULDING

One of the possible mechanisms for warpage formation is the buckling of injection-moulded articles resulting from improper ejection loads while samples were not stiff enough to bear the ejection stress. Estimation of the theoretical minimum cooling time necessary to allow mouldings to be cooled from a hot melting temperature to a temperature able to be demoulded has been conducted prior to the selection of the process variables and levels for the factorial experiment. For mouldings with a plate geometry, the minimum cooling time is given by:[1]

$$t_c = \frac{s^2}{\pi^2 a} \ln\left(\frac{8T_M - T_W}{\pi^2 T_D - T_W}\right) \qquad \text{(A1)}$$

where t_c is the cooling time; s is the wall thickness of the mouldings; a is the thermal diffusivity; T_M is the melt temperature; T_w is the moulding wall temperature and T_D is the average temperature across the sample thickness during demoulding. Equation (A1) is strictly valid for estimating the shortest cooling time for the plated samples, therefore, for samples with a parallelepiped geometry having a width to thickness ratio of 5:4 it may thus provide an upper bound for the required actual cooling time.

The thermal diffusivity, a, is calculated from $a = \kappa/\rho c_p$ where ρ is the density and c_p is the heat capacity. The Maxwell equation is employed for calculating the thermal conductivity (κ) of binary phases:

$$\kappa = \kappa_c \frac{1 + 2v_d(1 - \kappa_c/\kappa_d)/(2\kappa_c/\kappa_d + 1)}{1 - v_d(1 - \kappa_c/\kappa_d)/(\kappa_c/\kappa_d + 1)} \qquad \text{(A2)}$$

where κ_c and κ_d are thermal conductivities of the matrix and the dispersed phase, respectively; and v_d is the volume fraction of the dispersed phase.

Taking a mean thermal conductivity of zirconia as $1.81\,\mathrm{W\,mK^{-1}}$ across the temperature range used in this study and a thermal conductivity of $0.16\,\mathrm{W\,mK^{-1}}$ for the binder vehicles employed (note that the difference between thermal conductivities of 50:50 and 75:25 binder formulation is small and is thus treated equal), we thus find that the overall thermal conductivities for moulding materials of 50% and 57.5% solid loadings are 0.49 and $0.58\,\mathrm{W\,mK^{-1}}$, respectively. Notice that at both solid loadings, zirconia particles are assumed to be uniformly surrounded by the binder phases, i.e. there is a layer of binders separating the powders and hence the ceramic phase is considered to be the dispersed phase in eqn (A2) for both loadings. By using eqn (A1) and assuming T_D to be half of the difference between the melt temperature and the mould temperature, we thus find the shortest cooling time for the plasticated feedstock varies from 8.3 to 13.1 seconds for 57.5 and 50 vol% solid loadings, respectively. Strictly speaking, eqn (A2) is valid only for dilute case of binary mixtures. In addition, for the relatively low thermal conductivity materials used in this study, the interfacial resistance becomes more pronounced when the phonon's mean free path is small. Both reasonings reduce the conductivity and hence the thermal diffusivity, which in turn, increases the minimum cooling time. However, the powders form continuous paths (by, for example, powder agglomeration) in reality according to the percolation law as the filler fraction exceeds a certain critical limit. It hence leads to a higher conductivity since the zirconia ceramics presents a substantially higher value than those of the binder phases. Since the cooling times used in the experiment exceeded the calculated values, it is then reasonable to consider that the warpage of the mouldings did not result from the ejection forces at the prescribed experimental conditions.